に基づくもので、65歳以上の高齢者を対象に要介護の原因となりやすい生活機能低下の危険性がないかどうかという視点で運動、口腔、栄養、物忘れ、うつ症状、閉じこもり等の全25項目について「はい」「いいえ」で記入する質問表である。東浦町では基本チェックリストは平成21年度には、65歳以上の人口9,374人のうち、すでに要支援・要介護となっている者を除く8,091人の69.6%にあたる5,631人に実施された。3年半後には死亡者、転出者を除いて603名が要支援・要介護となった。多重ロジスティック回帰により性別、年齢を調整して要支援・要介護となるリスクについて検討を行った。項目別の検討ではチェックリスト項目すべてで有意となった(表1)。オッズ比が2倍以上となった項目は、「日用品の買い

表1　地域住民における3年半の追跡による基本チェック各項目の要支援・要介護となるリスクのオッズ比

項目	オッズ比	95%信頼区間	p値
バスや電車で1人で外出をしていない	1.99	1.64 − 2.41	p<0.001
日用品の買い物をしていない	2.34	1.83 − 3.00	p<0.001
預貯金の出し入れをしていない	1.80	1.44 − 2.26	p<0.001
友人の家を訪ねていない	1.83	1.51 − 2.20	p<0.001
家族の相談にのっていない	1.66	1.34 − 2.04	p<0.001
階段をつたわらずに昇れない	2.17	1.79 − 2.63	p<0.001
つかまらずに立てない	2.51	2.04 − 3.08	p<0.001
15分続けて歩くことはない	2.07	1.67 − 2.56	p<0.001
1年間に転んだことがある	2.05	1.66 − 2.55	p<0.001
転倒の不安が大きい	1.97	1.62 − 2.38	p<0.001
6ヵ月で3kgの体重減少	1.71	1.34 − 2.17	p<0.001
BMIが18.5未満	1.66	1.25 − 2.20	p<0.001
固いものが食べにくい	1.33	1.09 − 1.62	p=0.005
お茶でむせる	1.28	1.02 − 1.61	p=0.031
口の渇きが気になる	1.50	1.22 − 1.83	p<0.001
週に1回以上外出ない	1.70	1.29 − 2.24	p<0.001
昨年より外出回数が減少	2.31	1.90 − 2.82	p<0.001
物忘れがある	1.60	1.29 − 2.00	p<0.001
電話番号を調べてかけることはしない	2.35	1.80 − 3.07	p<0.001
今日の日付がわからない	1.85	1.52 − 2.25	p<0.001
生活に充実感がない	2.20	1.75 − 2.76	p<0.001
楽しめなくなった	2.64	2.04 − 3.41	p<0.001
おっくうに感じる	2.70	2.21 − 3.29	p<0.001
役に立つ人間だと思えない	2.16	1.76 − 2.65	p<0.001
疲れたような感じがする	1.95	1.60 − 2.38	p<0.001

(性別・年齢を調整した多重ロジスティック回帰解析)

物をしていない」、「階段をつたわらずに昇れない」、「つかまらずに立てない」、「15分続けて歩くことはない」、「1年間に転んだことがある」、「電話番号を調べてかけることをしない」、「昨年より外出回数が減少」、「生活に充実感がない」、「楽しめなくなった」、「おっくうに感じる」、「役に立つ人間だと思えない」であった。運動機能や抑うつに関連する項目でリスクが大きいことが分かる。基本チェックリストからの生活機能評価結果では、生活機能全般の障害が要支援・要介護の最大のリスクであり、オッズ比は4倍近くとなった。次いで運動機能障害、うつ状態、栄養状態の不良の順でリスクが大きかった（表2）。

2. 国立長寿医療研究センター・老化に関する長期縦断疫学研究

私たちは平成9年の11月に「国立長寿医療研究センター・老化に関する長期縦断疫学研究（NILS-LSA）」を開始した[3～5]。一日の検査人数は7名で、毎日年間を通して詳細な老化に関連する検査を行ってきた。平成12年4月に2,267名の基礎集団が完成し、以後は2年ごとに検査を繰り返し実施し、平成24年7月に第7次調査を終了した。対象者は長寿医療研究センター周辺在住の観察開始時年齢が40歳から79歳までの男女であり、地方自治体（大府市および東浦町）の協力を得て、地域住民から年齢・性別に層化した無作為抽出を行った。抽出によって選定された者を説明会に招いて、検査の目的や方法などを十分に説明し、インフォームドコンセントを得た上で検査を実施してきた。追跡中の80歳未満のドロップアウトは新たに無作為抽出を行い、同じ年齢、性別で新たな補充を行った。また、どの時点でも若い世代との比較ができるように無作為抽出で40歳の男女を毎回新たに加えて、定常状態として約2,400人のダイナミックコホートを目指してきた。検査および調査はほとんどすべて施設内に設けた専用の検査センターで行った。朝9時から夕方4時までの間に分刻みでスケジュールを組み、頭部MRI検査や心臓および頸動脈超音波断層検査、骨密度測定、腹部CT検査などの最新の機器を利用した医学検査のみならず、詳細な生活調査、栄養調査、運動機能調査、心理検査など広汎

表2　地域住民における3年半の追跡による基本チェックからの生活機能障害項目の要支援・要介護となるリスクのオッズ比

項目	オッズ比	95%信頼区間	p値
生活機能障害	3.82	3.05 － 4.78	p<0.001
運動機能障害	2.70	2.20 － 3.33	p<0.001
栄養状態の不良	2.44	1.31 － 4.54	p=0.005
口腔機能障害	1.59	1.27 － 1.99	p<0.001
閉じこもり	1.70	1.29 － 2.24	p<0.001
認知機能障害	1.80	1.50 － 2.15	p<0.001
うつ状態	2.54	2.09 － 3.09	p<0.001

（性別・年齢を調整した多重ロジスティック回帰解析、オッズ比は各項目1点ごとの値）

で学際的な、しかも精度の高い調査・検査を実施した。

要支援・要介護化の危険因子について、NILS-LSAの第4次調査から第7調査までの6年間に調査に参加した40歳以上の地域在住中高年者3,126人（男性1,567人、女性1,559人）を対象とした。平均年齢は、男性 58.4±13.2歳、女性 58.9±13.5歳である。

今回の検討に用いた測定項目は以下の通りである。

①背景要因：喫煙習慣（調査時点での喫煙の有無）、高血圧症、心疾患、脂質異常症、糖尿病、脳卒中既往歴、自覚的健康度（「とても良い」、「良い」、「普通」、「悪い」、「とても悪い」の5段階）、血圧、抑うつ（Center for Epidemilogic Studies Depression Scale: CES-Dで16点以上を抑うつありとした）、認知機能（Mini Mental State Examination: MMSEで23点以下を認知機能障害ありとした）。

②身体活動：余暇身体活動量、総身体活動量、一日歩数。

③体格：BMI、大腿中部周囲長、下腿周囲長、上腕周囲長、体脂肪率（DXA法）。

④栄養摂取量：総エネルギー摂取量、たんぱく質、ビタミンD、イソロイシン、ロイシン、バリン、アルギニン（写真撮影を併用した3日間の秤量食事記録法により栄養素の摂取量を算出した）。

⑤体力：普通歩速度、速歩速度、上体起こし、膝伸展筋力、脚伸展パワー、握力、閉眼片足立ち、開眼片足立ち、全身反応時間。

⑥身体機能：SF36のphysical performance項目。具体的な項目は以下の通りである。軽度：体を前に曲げる、百メートル以上歩く、中等度：適度の運動、階段を1階上まで登る、数百メートル以上歩く、高度：階段を数階上まで登る、激しい運動、少し重い物を運ぶ、1キロ以上歩く。これらの項目による得点が75点以下は要支援・要介護となる程度のADLの障害があると判定される。physical performanceが75点以下となる6年間のリスクを各種要因について、一般推定方程式（GEE）で性別・年齢を調整して推定し、オッズ比を計算した。

①生活習慣・背景要因などとADLの低下との関連

喫煙はADLの低下とは有意な関連はみられなかった。高血圧症、心疾患、脂質異常症、糖尿病、脳卒中の有無は疾患を有する群でADLが低下するリスクは高かった。自覚的健康度は、「良い」群に比べ「悪い」、「普通」の群はADL低下のリスクが有意に高かった。オッズ比は3.2と高い値であった。血圧は有意な結果とならなかった。抑うつはある群に比べてない群で有意にADL低下のリスクが低くなっていた。認知機能は認知機能低下がない群でADL低下のリスクが下がっていた（表3）。

②身体活動量、体力とADLの低下との関連

余暇身体活動量、総身体活動量、一日の歩数の身体活動指標はいずれも高いほどADL低下のリスクを下げていた。体力の指標では、握力、開眼片足立ち、閉眼片足立ち、全身反応時間、脚伸展パワー、上体起こし、膝伸展筋力、普通歩速度、速歩速度と体力指標すべてで成績が悪いとADL低下のリスクとなっていた（表4）。

③体格、栄養とADLの低下との関連

BMIは高くなるほどADL低下のリスクを上げていた。DXAで測定した体脂肪率は高いほどADL低下のリスクが高かった。しかし、大腿中部周囲長、下腿周囲長、上腕周囲長は

ADL低下との関連が認められなかった。エネルギー摂取量、たんぱく質摂取量、ビタミンD摂取量、イソロイシン摂取量、ロイシン摂取量、バリン摂取量、アルギニン摂取量、血清アルブミンの栄養の指標はすべてADL低下に関連しており、数値が低いとADL低下のリスクとなっていた（表5）。

ADL低下や虚弱の予防には多くのアプローチがあるが、NILS-LSAの解析から慢性疾患や抑うつの予防、十分に運動して、歩行能力や、体力を保つことが重要であることを確認することができた。

表3　生活習慣、背景要因などとADLの低下との関連

	項目	オッズ比	95%信頼区間	p値
喫煙	吸う vs 吸わない	1.070	0.796 – 1.437	NS
高血圧症	あり vs なし	1.564	1.324 – 1.846	<0.0001
心疾患	あり vs なし	1.768	1.329 – 2.352	<0.0001
脂質異常症	あり vs なし	1.266	1.055 – 1.521	0.0014
糖尿病	あり vs なし	1.739	1.321 – 2.291	<0.0001
脳卒中	あり vs なし	2.428	1.702 – 3.463	<0.0001
自覚的健康	普通・悪い vs 良い	3.198	2.659 – 3.846	<0.0001
収縮期血圧	10mmHgごと	1.031	0.990 – 1.074	NS
拡張期血圧	10mmHgごと	1.008	0.939 – 1.081	NS
抑うつ	CES-D 15以下 vs 16以上	0.468	0.391 – 0.560	<0.0001
認知機能	MMSE 24以上 vs 23以下	0.702	0.530 – 0.930	0.0136

SF36 physical performanceが75点以下となる6年間のリスクを各種要因について、一般推定方程式（GEE）で性別・年齢を調整し全対象者で推定し、オッズ比を計算した。

表4　身体活動量、体力とADLの低下との関連

	項目	オッズ比	95%信頼区間	p値
余暇身体活動量	100,000METS*min/yごと	0.518	0.408 – 0.658	<0.0001
総身体活動量	100,000METS*min/yごと	0.569	0.467 – 0.693	<0.0001
歩数	1000歩ごと	0.812	0.783 – 0.843	<0.0001
握力	10kgごと	0.377	0.307 – 0.462	<0.0001
開眼片足立ち	10秒ごと	0.942	0.923 – 0.962	<0.0001
閉眼片足立ち	10秒ごと	0.815	0.721 – 0.923	0.0012
全身反応時間	0.1秒ごと	1.371	1.256 – 1.496	<0.0001
脚伸展パワー	10Wごと	0.947	0.937 – 0.957	<0.0001
上体起こし	1回/分ごと	0.926	0.904 – 0.948	<0.0001
膝伸展筋力	10kgごと	0.522	0.455 – 0.599	<0.0001
普通歩速度	1m/分ごと	0.019	0.011 – 0.031	<0.0001
速歩速度	1m/分ごと	0.944	0.937 – 0.951	<0.0001

SF36 physical performanceが75点以下となる6年間のリスクを各種要因について、一般推定方程式（GEE）で性別・年齢を調整し全対象者で推定し、オッズ比を計算した。

3. 性別、加齢と自立障害

要支援・要介護は男性よりも女性に多い。平成24年度介護給付費実態調査の概況によれば、平成25年4月審査分においては、認定者数575万人、受給者数463万人となっており、受給者を性別にみると、男性が29.6%、女性が70.4% と女性が圧倒的に多くなっている。日本では平均寿命は女性の方が男性よりも7歳近く長い。寝たきりの期間も女性の方が長く、支援や介護を要する女性の数は男性よりも多い。年齢を調整しても要支援・要介護のリスクは男性よりも女性の方が高い[6]。また介護を要する女性の死亡率は男性よりも高いという報告もある[7]。

介護を要するような高齢者の虚弱は定義にもよるが、75歳以上の20〜30%に認められ、高齢になるほどその割合は高くなる[8]。多くの研究で、加齢は要介護の最も強い危険因子のひとつにあげられている。しかし、加齢そのものが要介護となる要因なのか、加齢に伴って生じる様々な障害や疾病が要因であって、これらの要因をすべて除いても加齢が要介護の要因であるかどうかについては、まだ十分には明らかにされていない。

4. 生活習慣と要介護

高齢者では一般に身体活動量が減り、また歯の脱落、嗅覚や味覚の低下、消化機能の低下など生理学的な要因に加えて、抑うつなどの精神的な要因のため食欲が低下する。こうした生活習慣の変化が、高齢者が要介護となる要因である可能性が高い。要介護となる栄養学的要因として低栄養、痩せが重要である。特に摂取エネルギー、蛋白質や必須アミノ酸摂取の低下、ビタミンやミネラル、特にビタ

表5　体格、栄養とADLの低下との関連

	項目	オッズ比	95%信頼区間	p値
BMI	1m/kg^{2}ごと	1.080	1.045 − 1.116	<0.0001
大腿中部周囲長	1cmごと	0.999	0.995 − 1.002	NS
下腿周囲長	1cmごと	0.993	0.980 − 1.005	NS
上腕周囲長	1cmごと	1.004	0.985 − 1.023	NS
体脂肪率（DXA）	10%ごと	1.782	1.470 − 2.160	<0.0001
エネルギー摂取量	100kcal/日ごと	0.940	0.918 − 0.963	<0.0001
たんぱく質摂取量	10g/日ごと	0.870	0.824 − 0.919	<0.0001
ビタミンD摂取量	5μg/日ごと	0.943	0.891 − 0.997	0.0379
イソロイシン摂取量	1g/日ごと	0.763	0.678 − 0.858	<0.0001
ロイシン摂取量	1g/日ごと	0.854	0.797 − 0.915	<0.0001
バリン摂取量	1g/日ごと	0.790	0.714 − 0.873	<0.0001
アルギニン摂取量	1g/日ごと	0.827	0.756 − 0.904	<0.0001
血清アルブミン	1g/dlごと	0.725	0.604 − 0.869	0.0005

SF36 physical performanceが75点以下となる6年間のリスクを各種要因について、一般推定方程式（GEE）で性別・年齢を調整し全対象者で推定し、オッズ比を計算した。

ミンD、カロテン、ビタミンB12、葉酸の摂取不足は高齢者の要介護と関連が深いと言われている[9]。前述したように、NILS-LSAでの検討でもこれらの栄養素の摂取とADLの低下の関連が明らかとなった。またNILS-LSAでは、体力はほとんどの項目でADL低下の予防因子であり、筋力、柔軟性、持久力、平衡機能、歩行能力のいずれもが重要であった。さらに身体活動量は余暇身体活動量、総身体活動量、一日歩数のいずれもが多いほどADL低下を予防するという結果であり、運動の重要性が確認された。

要介護となるような虚弱の栄養の指標としてアルブミン、コレステロールが使われてきた。横断的な解析では、低アルブミン血症（血清アルブミン3.5g/dl未満）は地域在住高齢者の身体機能やADL障害に関連していた[10,11]。縦断的研究では、3.8g/dl以下の低アルブミン血症が3年後の身体機能低下と関連していたが、7年後の身体機能低下とは関連をしていなかった。170 mg/dl未満の低コレステロール血症は死亡のリスクにはなっていたが、ADL低下のリスクにはなっていなかった[12]。コレステロールとアルブミンを組み合わせた縦断的な検討では、血清総コレステロールが5.2mmol/l（201mg/dl）以下で女性でのADL低下の危険因子となっていたが、血清アルブミンが4.3g/dl以下での判定では男女ともADL低下の危険因子とはならなかった。しかし、コレステロールとアルブミンの両方を組み合わせたところ、男性でのADL低下の危険因子となった[13]。HDLコレステロールについても施設入所の高齢者の2年間の追跡で、身体機能低下の重要なリスクファクターになっていることが示されている[14]。ADL低下と関連する栄養指標は、単独では見逃してしまうこともある。いくつかの指標を組み合わせて判断することも重要であろう。

高齢者のADLの低下に関しての大規模な縦断研究として米国の40,657人の65歳から79歳の女性を対象とした3年間の追跡研究Women's Health Initiative Observational Study（WHI-OS）がある[15]。WHI-OSではベースライン調査で16.3%が虚弱と判断され、さらに3年間の追跡で14.8%が新たに虚弱となった。ADL低下の要因として生活習慣についても詳細な調査が行われているが、その結果では喫煙はADL低下の危険因子であるが、飲酒は少量ならばむしろ予防するという結果が出ている。また、体重は低体重も肥満もともに正常体重に比べてADL低下の要因となっていた。喫煙はさまざまな慢性疾患の要因ではあるが、NILS-LSAでの検討では喫煙はADLの低下要因とはならなかった。6年間でADLの低下をきたすような集団はすでに喫煙を止めている可能性がある。また体格は東浦町の調査では体重減少や痩せは要支援・要介護の要因であったが、NILS-LSAでは体格はBMIや体脂肪率が多いほどADL低下を来しやすいという結果であり、痩せよりも肥満予防の重要性が示された。

5. 慢性疾患と要介護

WHI-OSの報告では慢性疾患やうつ症状が要介護や虚弱の要因であり、一方、自覚的健康度が高いことは虚弱を防ぐ要因であった。虚弱との関連が認められた慢性疾患は、冠動脈疾患、脳血管障害、糖尿病、高血圧症、大腿骨頸部骨折、慢性閉塞性肺疾患（COPD）、転倒、抑うつ、関節炎であった[15]。さらに認知症や認知機能障害が、高齢者の虚弱と関連

しているとする報告もある[16,17]。NILS-LSAでの調査では、高血圧症、心疾患、脂質異常症、糖尿病、脳卒中のような慢性疾患は程度の差はあるが、すべてADL低下の要因となっていた。自覚的健康度は良い場合に比べて、普通あるいは悪い場合にはADLの低下の強い要因であった。自己判断による健康状態がその後のADL低下を予測する要因であることは興味深い。また抑うつもADL低下の強い要因であった。しかし認知機能低下は有意ではあったが、ADL低下への影響はそれほど大きくはなかった。

慢性の炎症も要介護や虚弱の要因となる。IL-6が3.8 g/mlを超える場合、CRPが2.65 mg/lを超える場合には、3年間の追跡で有意に身体機能が低下していた[12]。男性ホルモンの低下についても、高齢男性の虚弱の要因であるとの報告がある。米国での1,469名の65歳以上高齢男性の検討では、血清テストステロン濃度が低いほど虚弱の割合が多く、4年間の縦断的追跡でも血清テストステロン濃度が低いほど虚弱となるリスクが高かった[18]。男性高齢者の場合、アンドロポーズと呼ばれる加齢に伴う男性ホルモンの低下が虚弱の要因として重要である。副腎や性腺で産生される男性ホルモンの一種であるデヒドロエピアンドロステロン（DHEA）も低値であることが高齢男女で虚弱と関連していた[19]。これら様々な慢性疾患や病態が重積することでさらに要介護や虚弱の危険が増加する。

6. 社会経済的要因と高齢者の要介護、虚弱

同じ定義を用いても、要介護、虚弱高齢者の分布には地域差があるといわれている。ヨーロッパ10カ国の調査では、65歳以上の虚弱高齢者の割合はスイスの5.8%からスペインの27.3%までと異なっており、同じヨーロッパでも概して南欧は北欧よりも虚弱な高齢者が多いとの結果であった[20]。この地域差には教育など社会経済的な要因が関与しているという。

米国のWHI-OSでは社会経済的要因として、世帯年収が高いほど、教育が長いほど、白人に比べむしろ黒人やアジア人でリスクが低かった[15]。また一人暮らしは虚弱となるリスクを20%下げていた。一人暮らしは、他の家族に依存できず自立が必要なためと思われる。一方で、3年間にわたる縦断的研究で、外出頻度が少ない、いわゆる「閉じこもり」で虚弱の発生率が高かったとの報告もある[21]。

7. 虚弱高齢者への介入研究

要介護や虚弱の予防を目指しての介入研究が繰り返し行われている。1994年にNew England Journal of Medicineに掲載されたFiataroneらによる虚弱高齢者への古典的な介入研究がある[22]。施設入所中の高齢者に対する無作為割付研究で筋肉トレーニングにより、虚弱の有意な改善が認められている。運動による介入の虚弱の改善効果については他の良くデザインされた研究でも認められているが[23]、否定的な結果の研究もある[24]。

栄養での介入でも虚弱の改善効果ははっきりしない。Fiataroneらによる無作為割付研究でのビタミン、ミネラル、蛋白質、脂質、炭水化物による栄養介入では、虚弱の改善効果は認められなかった[17]。必須アミノ酸である、バリン、ロイシン、イソロイシンの3つを分岐鎖アミノ酸という。筋肉を構成している必須アミノ酸の約35－40%がこの分岐鎖ア

ミノ酸であり、筋肉の蛋白質分解を抑制する。高齢者の筋量維持、増加にこの分岐鎖アミノ酸が有効だとする報告は多い[25]。しかし、実際に無作為割付研究を行っても、ロイシンをサプリメントとして3ヵ月間にわたって高齢男性に投与した介入試験では筋肉量や筋力への影響はなかったという[26]。この他にもビタミンDの投与による栄養介入の研究などもあるが[19]、虚弱の改善効果は認められていない。

おわりに

高齢者の要支援・要介護は年齢が高いほど割合が高くなり、また男性よりも女性で割合が高い。要介護の要因としては、低栄養、喫煙、慢性疾患への罹患、慢性炎症、性ホルモンの減少などの身体的要因に加えて、世帯の年収や教育歴、人種、生活空間など社会的な因子も重要である。高齢者ではこれらの多くの要因が重積し要介護状態を引き起こすものと考えられる。高齢者の虚弱に対しての運動や栄養による介入研究が数多く行われているが、その効果ははっきりしていない。運動介入や栄養の単独の介入では高齢者の要介護・虚弱の予防は難しく、生活全般のサポートでの対応が望まれる。

文　献

1）厚生統計協会（編）：国民衛生の動向．厚生の指標 2013/2014; 60: 76－79.

2）Muramatsu N, Akiyama H: Japan: super-aging society preparing for the future. Gerontologist. 2011; 51: 425－432.

3）下方浩史：長期縦断研究の目指すもの．Geriatric Medicine 1998; 36: 21－26.

4）Shimokata H, Ando F, Niino N: A new comprehensive study on aging - the National Institute for Longevity Sciences, Longitudinal Study of Aging (NILS-LSA). J Epidemiol 2000; 10: S1－S9.

5）下方浩史，安藤富士子：長期縦断疫学で分かったこと．日本老年医学会雑誌 2008; 45: 563－572.

6）Mor V, Wilcox V, Rakowski W, Hiris J: Functional transitions among the elderly: patterns, predictors, and related hospital use. Am J Public Health 1994; 84: 1274－1280.

7）Puts MT, Lips P, Deeg DJ: Sex differences in the risk of frailty for mortality independent of disability and chronic diseases. J Am Geriatr Soc 2005; 53: 40－47.

8）Topinkova E; Aging, disability and frailty. Ann Nutr Metab 2008; 52 (suppl 1), 6－11.

9）Bartali B, Frongillo EA, Bandinelli S, Lauretani F, Semba RD, Fried LP, Ferrucci L: Low nutrient intake is an essential component of frailty in older persons. J Gerontol A Biol Sci Med Sci 2006; 61: 589－593.

10）Salive ME, Cornoni-Huntley J, Phillips CL, Guralnik JM, Cohen HJ, Ostfeld AM, Wallace RB: Serum albumin in older persons: relationship with age and health status. J Clin Epidemiol 1992; 45: 213－221.

11）Jensen GL, Kita K, Fish J, Heydt D, Frey C. Nutrition risk screening characteristics of rural older persons: relation to functional limitations and health care charges. Am J Clin Nutr 1997; 66: 819－828.

12) Reuben DB, Cheh AI, Harris TB, Ferrucci L, Rowe JW, Tracy RP, Seeman TE.. Peripheral blood markers of in inflammation predict mortality and functional decline in high-functioning community-dwelling older persons. J Am Geriatr Soc 2002; 50: 638－644.
13) Schalk BW, Visser M, Deeg DJ, Bouter LM: Lower levels of serum albumin and total cholesterol and future decline in functional performance in older persons: the Longitudinal Aging Study Amsterdam. Age Ageing 2004; 33: 266－272.
14) Zuliani G, Romagnoni F, Bollini C, Leoci V, Soattin L, Fellin R. Low levels of high-density lipoprotein cholesterol are a marker of disability in the elderly. Gerontology 1999; 45: 317－322.
15) Woods NF, LaCroix AZ, Gray SL, Aragaki A, Cochrane BB, Brunner RL, Masaki K, Murray A, Newman AB; Women's Health Initiative: Frailty: emergence and consequences in women aged 65 and older in the Women's Health Initiative Observational Study. J Am Geriatr Soc 2005; 53: 1321－1330.
16) Black SA, Rush RD: Cognitive and functional decline in adults aged 75 and older. J Am Geriatr Soc 2002; 50: 1978－1986.
17) Buchman AS, Boyle PA, Wilson RS, Tang Y, Bennett DA: Frailty is associated with incident Alzheimer's disease and cognitive decline in the elderly. Psychosom Med 2007; 69: 483－489.
18) Cawthon PM, Ensrud KE, Laughlin GA, Cauley JA, Dam TT, Barrett-Connor E, Fink HA, Hoffman AR, Lau E, Lane NE, Stefanick ML, Cummings SR, Orwoll ES: Osteoporotic Fractures in Men (MrOS) Research Group: Sex hormones and frailty in older men: the osteoporotic fractures in men (MrOS) study. J Clin Endocrinol Metab 2009; 94: 3806－3815.
19) Voznesensky M, Walsh S, Dauser D, Brindisi J, Kenny AM: The association between dehydroepiandosterone and frailty in older men and women. Age Ageing 2009; 38: 401－406.
20) Santos-Eggimann B, Cuénoud P, Spagnoli J, Junod J: Prevalence of frailty in middle-aged and older community-dwelling Europeans living in 10 countries. J Gerontol A Biol Sci Med Sci 2009; 64: 675－681.
21) Xue QL, Fried LP, Glass TA, Laffan A, Chaves PH: Life-space constriction, development of frailty, and the competing risk of mortality: the Women's Health And Aging Study I. Am J Epidemiol 2008; 167, 240－248.
22) Fiatarone MA, O'Neill EF, Ryan ND, Clements KM, Solares GR, Nelson ME, Roberts SB, Kehayias JJ, Lipsitz LA, Evans WJ. Exercise training and nutritional supplementation for physical frailty in very elderly people. N Engl J Med 1994; 330: 1769－1775.
23) Gill TM, Baker DI, Gottschalk M, Peduzzi PN, Allore H, Byers A: A program to prevent functional decline in physically frail, elderly persons who live at home.N Engl J Med 2002; 347: 1068－1074.
24) Latham NK, Anderson CS, Lee A,

Bennett DA, Moseley A, Cameron ID: A randomized, controlled trial of quadriceps resistance exercise and vitamin D in frail older people: the Frailty Interventions Trial in Elderly Subjects (FITNESS). J Am Geriatr Soc 2003; 51, 291－299.
25) Fujita S, Volpi E: Amino acids and muscle loss with aging. J Nutr 2006; 136 (Suppl), 277S－280S.
26) Verhoeven S, Vanschoonbeek K, Verdijk LB, Koopman R, Wodzig WK, Dendale P, van Loon LJ: Long-term leucine supplementation does not increase muscle mass or strength in healthy elderly men. Am J Clin Nutr 2003; 89: 1468－1475.

Ann Nucl Med
DOI 10.1007/s12149-015-0948-8

ORIGINAL ARTICLE

Radiosynthesis and in vivo evaluation of two imidazopyridineacetamides, [^{11}C]CB184 and [^{11}C]CB190, as a PET tracer for 18 kDa translocator protein: direct comparison with [^{11}C](*R*)-PK11195

Kentaro Hatano · Katsuhiko Sekimata · Takashi Yamada · Junichiro Abe · Kengo Ito · Mikako Ogawa · Yasuhiro Magata · Jun Toyohara · Kiichi Ishiwata · Giovanni Biggio · Mariangela Serra · Valentino Laquintana · Nunzio Denora · Andrea Latrofa · Giuseppe Trapani · Gaetano Liso · Hiromi Suzuki · Makoto Sawada · Masahiko Nomura · Hiroshi Toyama

Received: 27 June 2014 / Accepted: 14 January 2015

Abstract

Objective We report synthesis of two carbon-11 labeled imidazopyridines TSPO ligands, [^{11}C]CB184 and [^{11}C]CB190, for PET imaging of inflammatory process along with neurodegeneration, ischemia or brain tumor. Biodistribution of these compounds was compared with that of [^{11}C]CB148 and [^{11}C](*R*)-PK11195.

Methods Both [^{11}C]CB184 and [^{11}C]CB190 having ^{11}C-methoxyl group on an aromatic ring were readily prepared using [^{11}C]methyl triflate. Biodistribution and metabolism of the compounds were examined with normal mice. An animal PET study using 6-hydroxydopamine treated rats as a model of neurodegeneration was pursued for proper estimation of feasibility of the radioligands to determine neuroinflammation process.

Results [^{11}C]CB184 and [^{11}C]CB190 were obtained via *O*-methylation of corresponding desmethyl precursor using [^{11}C]methyl triflate in radiochemical yield of 73 % (decay-corrected). In vivo validation as a TSPO radioligand was carried out using normal mice and lesioned rats. In mice, [^{11}C]CB184 showed more uptake and specific binding than [^{11}C]CB190. Metabolism studies showed that 36 % and 25 % of radioactivity in plasma remained unchanged 30 min after intravenous injection of [^{11}C]CB184 and [^{11}C]CB190, respectively. In the PET study using rats, lesioned side of the brain showed significantly higher uptake than contralateral side after i.v. injection of either [^{11}C]CB184 or [^{11}C](*R*)-PK11195. Indirect Logan plot analysis revealed distribution volume ratio (DVR) between the two sides which might indicate lesion-related elevation of TSPO binding. The DVR was 1.15 ± 0.10 for [^{11}C](*R*)-PK11195 and was 1.15 ± 0.09 for [^{11}C]CB184.

Conclusion The sensitivity to detect neuroinflammation activity was similar for [^{11}C]CB184 and [^{11}C](*R*)-PK11195.

K. Hatano · K. Sekimata · T. Yamada · J. Abe · K. Ito
Department of Clinical and Experimental Neuroimaging, Center for Development of Advanced Medicine for Dementia, National Center for Geriatrics and Gerontology, Obu, Aichi 474-8522, Japan

Present Address:
K. Hatano (✉)
Faculty of Medicine, University of Tsukuba, Tsukuba 305-8575, Japan
e-mail: hatanok@md.tsukuba.ac.jp

M. Ogawa · Y. Magata
Medical Photonics Research Center, Hamamatsu University School of Medicine, Hamamatsu, Shizuoka 431-3192, Japan

J. Toyohara · K. Ishiwata
Research Team for Neuroimaging, Tokyo Metropolitan Institute of Gerontology, Tokyo 173-0015, Japan

G. Biggio · M. Serra
Department of Experimental Biology, University of Cagliari, 09100 Cagliari, Italy

V. Laquintana · N. Denora · A. Latrofa · G. Trapani · G. Liso
Pharmaco-Chemistry Department, University of Bari, Via Orabona 4, 70125 Bari, Italy

H. Suzuki · M. Sawada
Research Institute of Environmental Medicine, Nagoya University, Nagoya, Aichi 464-8601, Japan

M. Nomura · H. Toyama
Department of Radiology, Fujita Health University, Toyoake, Aichi 470-1192, Japan

Published online: 24 January 2015

Keywords Positron emission tomography · TSPO · PBR · Neuroinflammation · Alzheimer's disease

Introduction

Translocator protein (18 kDa) (TSPO) formerly referred to as peripheral benzodiazepine receptor (PBR) is a transmembrane multimeric protein complex primarily located in the outer mitochondrial membrane of cells [1]. It is especially concentrated in the outer/inner mitochondrial membrane contact sites [2], where it has been suggested to form a complex with other proteins such as the voltage-dependent anion channel and the adenine nucleotide transporter [3, 4]. TSPO is involved in various cell functions including porphyrin transport, heme biosynthesis, cholesterol transport, cell proliferation, apoptosis and anion transport [reviewed in 5, 6]. In central nervous system (CNS), TSPO is considered an ideal marker molecule for microglia activation [7]. Microglia undergo changes from a resting to an activated phenotype in response to a wide variety of CNS insults such as infectious diseases, inflammation, trauma, ischemia, brain tumors and neurodegeneration [8, 9]. Accumulation of a TSPO radioligand in lesioned area of brain is believed to be related with this microglia activation, and this is a key concept of clinical imaging of degenerative disorders of brain such as Alzheimer's disease by the means of positron emission tomography (PET) and this type of radioligand [7]. Our group reported that uptake of a TSPO radioligand, [^{11}C](*R*)-PK11195 was more related to this activation than number of the microglia cells [10] and suggested unknown mechanisms underlying the facilitated uptake of a TSPO radioligand.

[^{11}C](*R*)-PK11195 was the first TSPO radioligand applied to CNS diseases involving neuroinflammation process with PET [11]. Many clinical brain imaging studies were reported [reviewed in 8], however, the high degree of nonspecific uptake of [^{11}C](*R*)-PK11195 complicates the quantification and modeling of the PET data [12–15]. This significantly limits its sensitivity in detecting brain disorders. In this consequence, numerous radioligands for TSPO have been reported (Fig. 1). Zhang first reported carbon-11 labeled phenoxyphenyl acetamide, DAA1106 [16] and its fluoroalkyl congeners [17]. Briard reported structurally related phenoxypyridinyl acetamide, [^{11}C]PBR28 [18] and later Wilson also offered its fluoroalkyl congener, [^{18}F]FEPPA [19]. Another structural category should be referred to as "heterocyclic acetamide". Kassiou and coworkers reported pyrazolopyrimidinyl acetamides, [^{11}C]DPA-713 [20] and [^{18}F]DPA-714 [21]. Another example was dihydropurinylacetamide, [^{11}C]AC-5216 contributed by Zhang et al. [22]. Mattner offered I-123 labeled imidazopyridineacetamide, [^{123}I]CLINDE, for single photon emission computed tomography imaging [23].

We also reported four compounds of this class [24]. Only compound **[^{11}C]7** in the paper which is currently renamed as [^{11}C]CB148 showed satisfactory performance as a TSPO ligand in vivo. In the present article we report another two imidazopyridines, [^{11}C]CB184 and [^{11}C]CB190, with an ^{11}C-methoxyl group on an aromatic ring (Fig. 2). Feasibility of the compounds was examined

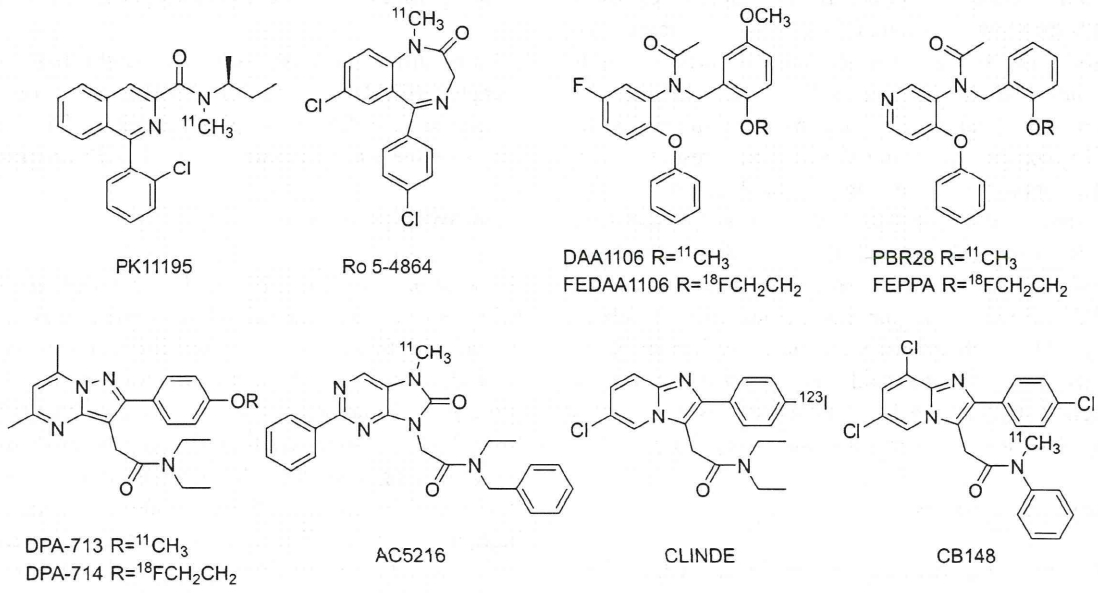

Fig. 1 Structures of TSPO radioligands

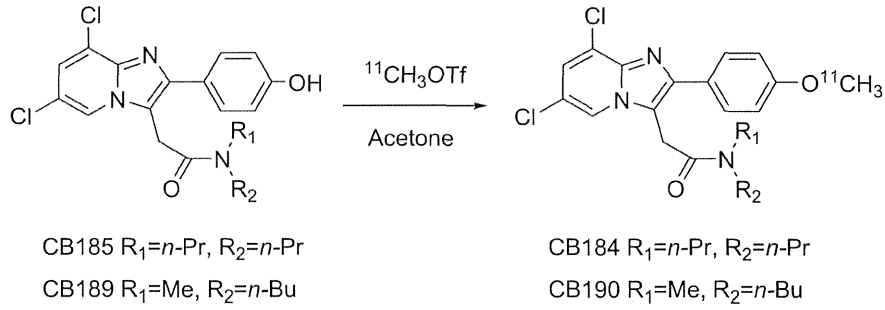

CB185 R_1=*n*-Pr, R_2=*n*-Pr

CB189 R_1=Me, R_2=*n*-Bu

CB184 R_1=*n*-Pr, R_2=*n*-Pr

CB190 R_1=Me, R_2=*n*-Bu

Fig. 2 Scheme of radiosynthesis

using intact mice following our previous report. In addition to this, we employed rat injury model of neurodegenerative disease. Measurement using high resolution animal PET and precise posthumous examination of the animals would reveal relevance of the methodology as well as the feasibility of the compounds in more persuasive manner, although there exist some difficulties pursuing this type of animal model study such as measurement and quantification method or appropriateness of the animal employed as human disease model. This study indicates proper direction for examining TSPO ligand performance.

Materials and methods

General

Reverse-phase high performance liquid chromatography (HPLC) was performed using LC-10A HPLC system (Shimadzu, Kyoto, Japan) accompanied by gamma ray detection using a NaI (Tl) scintillation system. An automated gamma counter with a NaI (Tl) detector (COBRA, Packard Instrument, Meriden, CT) was used to measure the radioactivity of samples from animal and partition coefficient studies. Male ddY mice and Wistar rats were supplied by Japan SLC (Hamamatsu, Japan) and Nihon Charles River (Tokyo, Japan), respectively. The present animal study was approved by the institutional committees for animal studies. Racemic PK11195 was purchased from Sigma (St. Louis, MO) and 0.1 M lithium aluminum hydride solution in tetrahydrofuran and a desmethyl derivative of (*R*)-PK11195 was purchased from ABX (Radeberg, Germany). Other chemicals were purchased from Kanto Chemicals (Tokyo, Japan) and were of the highest grade commercially available. All statistical analyses were carried out using StatView (SAS Institute Inc., Cary, NC).

Radiochemical syntheses

Unlabeled reference standard of CB184 and CB190 and their precursors, CB185 and CB189 were prepared according to previously reported method [25]. Carbon-11 was produced by $^{14}N(p, \alpha)^{11}C$ nuclear reaction using a CYPRIS HM18 cyclotron (Sumitomo Heavy Industries, Tokyo, Japan). [^{11}C]CO_2 thus obtained was converted to [^{11}C]methyl triflate using an automated synthesis system (CUPID C-11-BII, Sumitomo Heavy Industries, Tokyo, Japan). The obtained [^{11}C]methyl triflate was trapped in 0.3 mL acetone solution of containing 1 mg of CB185 or CB189 and 0.4 mg of NaOH (Fig. 3). The mixture was then heated at 80 °C for 3 min allowing the methylation reaction to occur. HPLC fractions containing purified [^{11}C]CB184 or [^{11}C]CB190 were collected into an evaporating vessel (HPLC conditions are summarized in Table 1). After removal of solvent, the residue was redissolved in the appropriate solvent and analyzed by reverse-phase HPLC (Table 1). The specific radioactivity of compounds was calculated by comparing the injected radioactivity with the corresponding UV peak area at 250 nm. Radiochemical synthesis of [^{11}C](*R*)-PK11195 was reported elsewhere [26].

Binding affinity and octanol/water partition coefficient

Binding affinity toward TSPO and central benzodiazepine receptor (CBR) and partition coefficient (Log *P*) were measured according to our previous report [24]. Separately, Log *P* value was calculated with CLOGP program [24].

Biodistribution in mice

A solution of [^{11}C]CB184, [^{11}C]CB190 or [^{11}C](*R*)-PK11195 in physiological saline containing 0.25 % polysorbate 80 (4 MBq/0.1 mL, 60–180 ng) was injected in male ddY mice (8–10 weeks old, 33–38 g, $n = 4$ for each group) via the tail vein. The mice were euthanized at 1, 15, 30 and 60 min after injection. Blood was removed by heart puncture using a syringe. Brain was dissected into olfactory bulb, cerebral cortex, striatum, thalamus, midbrain, cerebellum, and pons. The organs and the brain areas were weighed and the radioactivity was measured with a gamma counter. The raw counts were decay corrected to a standard

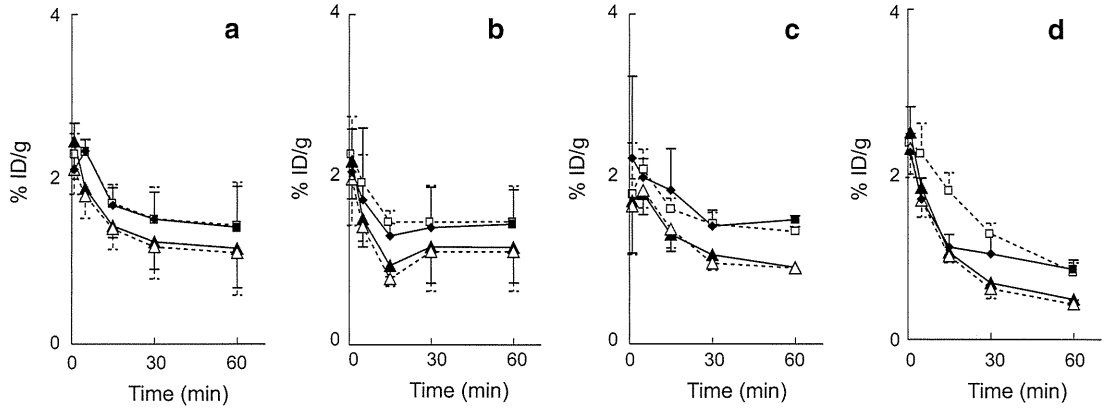

Fig. 3 Regional brain distribution; regional brain distribution of radioactivity after tail-vein injection of [^{11}C]CB184, [^{11}C]CB190, [^{11}C]CB148 and [^{11}C](*R*)-PK11195 in ddY mice is shown in **a–d**, respectively. Data are expressed as percentage of the injected dose per gram of tissue (%ID/g, mean and SD of four animals). *open circle* cerebellum, *filled circle* thalamus, *open triangle* cortex, *filled triangle* olfactory bulb. Data of [^{11}C]CB148 (**c**) was taken from literature [24]

Table 1 HPLC conditions

Compound	Eluent	Flow rate (mL/min)	Retention time (min)
Preparative			
CB184	Acetonitrile:H_2O (6:4)	6	9.1
CB190	Acetonitrile:H_2O (55:45)	6	10.1
Analytical			
CB185	Acetonitrile:H_2O (7:3)	1	7.8
CB190	Acetonitrile:H_2O (65:35)	1	8.0

Conditions employed for preparative and analytical HPLC are shown. Preparative HPLC was carried out using a Capcellpak C18 UG120S-5 μm column (10 mm inner diameter (i.d.) × 250 mm, Shiseido, Tokyo, Japan) and a JASCO HPLC system (JASCO, Tokyo, Japan) installed within the radiosynthesis system. Analytical HPLC was conducted using a Capcellpak C18 UG120S-5 μm column (4.8 mm i.d. × 250 mm, Shiseido, Tokyo, Japan) and a Shimadzu HPLC system (Shimadzu, Kyoto, Japan) with gamma ray detection using NaI(Tl) scintillator

time and the results were expressed as percentage of the injected does per gram of tissue (%ID/g).

Blocking studies

Mice (9–10 weeks old, 35–38 g, $n = 4$) were given via the tail vein with 0.1 mL of PK11195 in DMSO or flumazenil in physiological saline. All drugs were administered at dose of 1 mg/kg. A solution of each radioligand (prepared as above, 4 MBq/0.1 mL, 60–170 ng) was injected at 1 min after the cold drug treatment. At 30 min post-injection of the radioligand, the mice were euthanized and processed to measure %ID/g as above. Data were analyzed one-way ANOVA with Bonferroni's correction. Differences were considered significant at a p value less than 0.0167.

Metabolite studies

[^{11}C]CB184 or [^{11}C]CB190 (50–167 MBq, 0.46–1.1 μg) was intravenously injected into mice (8–9 weeks old, 36–39 g, $n = 3$ for each tracer), and 30 min later they were killed by cervical dislocation. Blood was removed by heart puncture using a heparinized syringe, and the brain was removed. After centrifugation of the blood at 7,000×g for 1 min at 4 °C the plasma of obtained, and 0.2–0.3 mL of the plasma was diluted with water up to 0.5 mL and denatured with 0.5 mL of acetonitrile in an ice-water bath. The suspension of plasma was centrifuged in the same condition and divided into soluble and precipitable fractions. The precipitate was re-suspended in 0.5 ml of acetonitrile followed by centrifugation. This procedure was repeated twice. The cerebellum (61–80 mg) was homogenized in 1 mL of a mixture of acetonitrile/water (1/1, v/v). The homogenate was treated as described above. Radioactivity in the three soluble fractions and precipitates was measured with gamma counter. In this treatment, the recovery yields in the soluble fraction were 80.3 ± 3.3 and 99.6 ± 0.1 % for plasma and brain, respectively, of mice given [^{11}C]CB184, and 96.6 ± 3.3 and 99.7 ± 0.3 % for plasma and brain, respectively, of mice given [^{11}C]CB190. The soluble fractions were combined and centrifuged as described above. A portion of the supernatant was analyzed by HPLC with a radioactivity detector (Radiomatic 150TR, Packard, Meriden, CT). A YMC-Pack ODS-A column (10 mm inner diameter (i.d.) × 150 mm, YMC, Kyoto, Japan) was used with acetonitrile/50 mM acetic acid/50 mM sodium acetate, pH 4.5 (80/10/10, v/v) at a flow rate of 2 mL/min. The retention times of [^{11}C]CB184 and [^{11}C]CB190 were 10.7 and 9.2 min, respectively. The recovery in the eluate of the injected radioactivity was essentially quantitative.

PET study

Using male Wistar rats (270–370 g), general anesthesia was induced by administering pentobarbital (50 mg/kg). After immobilizing the head using a brain stereotactic apparatus (Narishige, Tokyo, Japan), an incision was placed on the scalp to expose the skull. Using a bone drill, a hole was made in the skull to an area that was 0.4 mm anterior, 3 mm lateral, and 4.5 mm ventral to the bregma (point on the skull where the coronal and sagittal sutures converge), and solution of 6-hydroxydopamine (6-OHDA, 10 μg, Sigma-Aldrich, St. Louis, MO) in 2.5 μL physiological saline was directly injected into the right striatum [26].

Four days after the operation, the rat was anesthetized by 2 % isoflurane in O_2 (2 L/min) and placed in PET gantry of animal PET/CT system (FX-3200, Gamma Medica-Ideas, Northridge, CF) [27]. [^{11}C]CB184 or [^{11}C](*R*)-PK11195 was injected through tail vain and list-mode PET scan was carried out for 60 min. Scans by the radioligands with high and low specific radioactivity were available as we tried serial two scans from one batch of the each tracer. Injected dose is summarized in Table 5. CT data were obtained after the completion of PET acquisition. PET images were reconstructed using 3D maximum likelihood expectation maximization (MLEM) algorithm. Regions of interest (ROIs) were placed on right or left stratum with the aid of superimposed CT scull images using PMOD (PMOD Technologies, Zuerich, Switzerland). Data were expressed in standardized uptake value (SUV).

Time-activity curve (TAC) thus obtained was analyzed by indirect Logan plot method as reported by Converse [28, 29] for [^{11}C](*R*)-PK111195 employing uptake of the lesioned side as target and the contralateral side as reference. The same method was also applied to [^{11}C]CB184 in this study. The slope of the plot derives distribution volume ratio (DVR)—the ratio of distribution volume of right (6-OHDA lesioned) stratum to distribution volume of left stratum. Data were analyzed one-way ANOVA with Bonferroni's correction. Differences were considered significant at a p value less than 0.0083.

Histochemical examination

After euthanasia of the rat used in PET experiment, brain was removed and perfused for histological evaluation according to our report [10]. Numbers of tyrosine hydroxylase (TH) positive neurons were counted. Expression of mRNA coding tumor necrosis factor α (TNF-α) and interleukin-1β (IL-1β) was quantified using a RT-PCR method which was normalized by expression of NADPH [10]. Correlation between histochemistry and PET DVR was examined with Fisher's transformation which derived correlation coefficient (R) and critical value (p).

Table 2 Receptor binding affinity and partition coefficient

K_i (nM)			Log *P*	
Compound	TSPO	CBR	Calculated	Measured
CB148	0.203[a]	6880[a]	5.88[a]	2.20 ± 0.06[a]
CB184	0.537	>10000	4.99	2.06 ± 0.02[b]
CB190	0.882	>10000	3.93	2.39 ± 0.03[b]
(*R*)-PK11195	4.269[a]	7590[a]		2.54 ± 0.05[a]

[a] Data from literature [24]

[b] Mean ± SD of three runs

Results

Binding affinity octanol/water partition coefficient

Binding affinity of CB184, CB190, CB148 and (*R*)-PK11195 toward TSPO and CBR are shown in Table 2. Calculated and measured Log P values were also tabulated. Three CB compounds showed from 4.8 to 21 times higher affinity toward TSPO than (*R*)-PK11195. Selectivity of CB184 and CB190 was also higher than the other two. Especially, binding of CB184 or CB190 to CBR was under detectable range. Measured Log *P* values were similar among CB compounds, however, calculated Log *P* values were different from measured values as we previously reported [24].

Radiochemistry

Radiosynthesis of [^{11}C]CB184 and [^{11}C]CB190 could be achieved with [^{11}C]methyl triflate and acetone as reaction solvent. Decay-corrected radiochemical yield was 73 ± 12 % (n = 8) based on total [^{11}C]methyl triflate used in the synthesis and no difference between two compounds was observed. Time required for synthesis was 34 ± 2 min from the end of irradiation. The specific radioactivity was 184 ± 80 GBq/μmol (n = 8) at the end of synthesis, and the radiochemical purity was over 95 %.

Distribution of [^{11}C]CB184 and [^{11}C]CB190 in organs and brain regions

The organ distribution of radioligands was determined (Table 3) after tail vein injection of [^{11}C]CB184, [^{11}C]CB190 or [^{11}C](*R*)-PK11195. A high initial concentration of radioactivity was found in the lung, heart, and kidney. In Fig. 3, [^{11}C]CB184 and [^{11}C]CB190 showed similar time courses of regional brain distribution as [^{11}C]CB148 in the same experimental system [24]. The cerebellum and olfactory bulb showed more uptake than the other brain regions. [^{11}C](*R*)-PK11195 cleared more rapidly than three CB compounds.

Table 3 Organ distribution of radioactivity after intravenous injection of [^{11}C]CB184 and [^{11}C]CB190 into mice

Organ	Time after injection (min)				
	1	5	15	30	60
[^{11}C]CB184 uptake (%ID/g)					
Blood	5.14 ± 0.33	3.41 ± 0.56	1.51 ± 0.23	0.96 ± 0.26	0.64 ± 0.08
Heart	13.23 ± 1.44	12.34 ± 2.52	13.18 ± 5.51	13.83 ± 2.08	7.72 ± 1.69
Lung	94.82 ± 33.08	54.35 ± 15.27	25.30 ± 14.71	33.19 ± 18.49	13.82 ± 2.33
Liver	2.06 ± 3.31	9.81 ± 4.52	11.15 ± 7.75	2.69 ± 0.94	6.66 ± 1.75
Pancreas	3.66 ± 0.88	4.28 ± 1.40	5.49 ± 0.98	3.00 ± 0.87	3.57 ± 0.82
Spleen	4.12 ± 1.80	19.58 ± 6.59	13.78 ± 0.89	6.51 ± 2.13	10.08 ± 0.50
Kidney	9.04 ± 1.67	13.06 ± 2.68	42.55 ± 32.24	10.99 ± 1.93	11.69 ± 2.56
Intestine	4.47 ± 0.88	6.33 ± 2.91	3.58 ± 1.89	8.07 ± 4.84	5.08 ± 1.87
Testis	0.63 ± 0.41	1.10 ± 0.61	0.70 ± 0.30	0.58 ± 0.17	0.73 ± 0.09
[^{11}C]CB190 uptake (%ID/g)					
Blood	3.73 ± 0.83	2.42 ± 1.20	1.03 ± 0.22	0.70 ± 0.0.13	0.59 ± 0.10
Heart	15.03 ± 2.17	14.45 ± 1.85	11.74 ± 1.78	9.84 ± 1.84	10.55 ± 7.26
Lung	84.23 ± 28.14	42.18 ± 15.34	27.61 ± 6.57	19.39 ± 3.16	51.52 ± 29.19
Liver	2.65 ± 0.58	3.04 ± 0.31	5.46 ± 1.17	5.10 ± 0.77	2.09 ± 1.32
Pancreas	4.08 ± 1.23	4.40 ± 0.57	5.15 ± 0.46	4.78 ± 1.29	3.24 ± 1.74
Spleen	3.95 ± 1.39	7.59 ± 1.85	11.05 ± 2.47	11.64 ± 1.49	4.31 ± 3.12
Kidney	10.60 ± 3.43	12.92 ± 2.46	17.51 ± 0.56	15.04 ± 2.77	8.98 ± 4.94
Intestine	4.43 ± 0.55	5.47 ± 1.10	4.93 ± 1.64	3.87 ± 2.11	3.48 ± 2.59
Testis	0.86 ± 0.55	0.95 ± 0.20	1.06 ± 0.27	0.94 ± 0.15	0.62 ± 0.46

Data represent mean ± SD of four animals

Blocking studies

In vivo selectivity and specificity of [^{11}C]CB184 and [^{11}C]CB190 were examined by pretreatment with PK11195 or flumazenil. Uptake of the each radioligand in brain regions was measured at 30 min post-injection as the uptake levels were observed almost stable from 30 to 60 min post-injection. The uptake of [^{11}C]CB184 was significantly reduced relative to controls in every brain region by PK11195 (Table 4). Flumazenil had little effect on the uptake. In contrast, high uptakes of [^{11}C]CB190 in the cerebellum and olfactory bulb were significantly decreased along with PK11195 treatment, however, the other brain regions did not show the reduction. Similarly, inhibition of [^{11}C](*R*)-PK11195 uptake by cold PK11195 could not be observed in the pons and thalamus.

Metabolite studies

In HPLC analysis of plasma of mice given [^{11}C]CB184, two major radioactive peaks with the retention times of 3.5 and 5.7 min were detected except for [^{11}C]CB184 (retention time of 10.7 min). In the case of [^{11}C]CB190 (retention time 9.2 min), two major radioactive peaks were also found in the retention times of 3.5 and 5.5 min, and several minor metabolites were detected between 2.2 and 3.5 min. In the brain, the radioactive peaks in the retention times of 3.5 min were also found in addition to unchanged form of both tracers. At 30 min after injection of tracer, the percentages of the unchanged form in the brain and plasma were 92.7 ± 5.8 and 36.2 ± 15.5 %, respectively, for [^{11}C]CB184, and the corresponding figures for [^{11}C]CB190 were 86.5 ± 2.8 and 25.6 ± 7.1 %.

Animal PET studies

Time-activity curve after intravenous injection of [^{11}C](*R*)-PK11195 or [^{11}C]CB184 are shown in Fig. 4. Right and left striatum showed similar TACs when radioligands were injected in control animals (Fig. 4a, c). In contrast, 6-OHDA lesion resulted in increased uptake of both radioligands in lesioned side compared to contralateral side (Fig. 4b, d). Visual inspection revealed [^{11}C](*R*)-PK11195 was cleared more rapidly than [^{11}C]CB184. Although we tried serial two PET scans from one batch of the each tracer, the difference of pharmacological dose between low and high dose groups (Table 5) did not affect striatal uptake of both tracers (data are not shown). TACs thus obtained were analyzed by an indirect Logan plot method as reported by Converse for [^{11}C](*R*)-PK11195 employing uptake of the lesioned side as target and the contralateral side as Reference [28, 29]. Figure 5 shows satisfactory linear fitting of [^{11}C](*R*)-PK11195 or [^{11}C]CB184 in both control and lesioned animals. DVRs of [^{11}C](*R*)-PK11195

Table 4 Regional brain distribution of [^{11}C]CB184, [^{11}C]CB190 and [^{11}C](*R*)-PK11195 in mice after treatment with unlabeled drugs

Region	Injected drug		
	Control	PK11195	Flumazenil
[^{11}C]CB184 uptake (%ID/g)			
Olfactory bulb	1.45 ± 0.03	0.92 ± 0.11*	1.36 ± 0.30
Cortex	0.986 ± 0.073	0.594 ± 0.037*	0.965 ± 0.075
Striatum	0.864 ± 0.135	0.616 ± 0.026	0.806 ± 0.141
Hippocampus	1.225 ± 0.067	0.659 ± 0.099*	1.087 ± 0.122
Thalamus	0.985 ± 0.042	0.625 ± 0.024*	0.908 ± 0.159
Midbrain	0.965 ± 0.071	0.626 ± 0.031*	0.994 ± 0.228
Cerebellum	1.384 ± 0.091	0.729 ± 0.057*	1.361 ± 0.185
Pons	1.045 ± 0.102	0.655 ± 0.045*	1.003 ± 0.180
[^{11}C]CB190 uptake (%ID/g)			
Olfactory bulb	1.434 ± 0.090	1.026 ± 0.277*	1.329 ± 0.183
Cortex	0.838 ± 0.072	0.731 ± 0.227	0.722 ± 0.080
Striatum	0.715 ± 0.052	0.738 ± 0.235	0.704 ± 0.115
Hippocampus	0.887 ± 0.171	0.763 ± 0.134	0.643 ± 0.083
Thalamus	0.761 ± 0.084	0.702 ± 0.220	0.718 ± 0.097
Midbrain	0.950 ± 0.062	0.781 ± 0.214	0.830 ± 0.313
Cerebellum	1.363 ± 0.046	0.849 ± 0.232*	1.223 ± 0.275
Pons	0.890 ± 0.076	0.682 ± 0.199	0.793 ± 0.122
[^{11}C](*R*)-PK11195 uptake (%ID/g)			
Olfactory bulb	1.129 ± 0.107	0.481 ± 0.240*	1.015 ± 0.218
Cortex	0.626 ± 0.191	0.409 ± 0.112	0.606 ± 0.048
Striatum	0.507 ± 0.090	0.308 ± 0.089	0.634 ± 0.205
Hippocampus	0.730 ± 0.225	0.390 ± 0.054	0.746 ± 0.248
Thalamus	0.578 ± 0.297	0.431 ± 0.205	0.456 ± 0.068
Midbrain	0.610 ± 0.056	0.359 ± 0.052*	0.648 ± 0.134
Cerebellum	1.230 ± 0.243	0.389 ± 0.025*	1.171 ± 0.222
Pons	1.129 ± 0.107	0.481 ± 0.240	1.015 ± 0.218

Data represent mean ± SD of four animals. Blocking drugs were intravenously injected 1 min prior to the tracer administration. Data were analyzed 1-way ANOVA with Bonferroni's correction. Differences were considered significant at a p value less than 0.0167 (*)

in control and lesioned animals were 1.02 ± 0.08 ($n = 4$) and 1.15 ± 0.10 ($n = 5$), respectively, (mean ± SD). DVRs for [^{11}C]CB184 in control and lesioned animals were 1.03 ± 0.03 ($n = 4$) and 1.15 ± 0.09 ($n = 6$), respectively. Both radioligands showed significantly different DVR values between control and lesioned rats.

Correlations between the DVR values for [^{11}C](*R*)-PK11195 or [^{11}C]CB184 and histochemical data were examined. Data for both control and 6-OHDA treated rats are plotted in Fig. 6. Significant correlation ($p < 0.05$) was only seen between [^{11}C](*R*)-PK11195 and TH (Fig. 6a). Correlation between [^{11}C]CB184 and TH (Fig. 6d, $p = 0.06$) was not statistically significant, however, this would be expected with increasing number of data. The tendencies of positive correlation between DVR of [^{11}C](*R*)-PK11195 or [^{11}C]CB184 and expression of TNFα or IL-1β expression were also observed in spite they lack statistical significance (Fig. 6b, c, e, f).

Discussion

We previously reported preparation and biodistribution of four TSPO radioligands with imidazopyridineacetamide structure [24] via *N*-[^{11}C]methylation reaction. Among those, only [^{11}C]CB148 (compound **[^{11}C]7** in the previous paper) showed positive results. We are presenting herewith two another compounds of this class, [^{11}C]CB184 and [^{11}C]CB190. Radiosynthesis of these novel compounds is quite straightforward. Using [^{11}C]methyl triflate, these compounds were obtained with radiochemical yield of 73 % (decay-corrected). *O*-[^{11}C]Methylation of the phenolic hydroxyl group in the presence of small amount of NaOH should be regarded as the first choice in labeling strategy.

In vivo validation as a TSPO radioligand was firstly carried out following our previous report using normal mice [24]. In addition, an animal PET study using 6-OHDA treated rats as a model of neurodegeneration was pursued for proper estimation of feasibility of the radioligands to determine neuroinflammation process. In mice, among the brain regions examined, cerebellum and olfactory bulb showed the highest uptake of the every tracer examined. Even in normal rodents, microglia cells are present in all major divisions of brain [30]. Higher density of TSPO in the olfactory bulb of normal rodents is consistent across publications, however, TSPO density in the cerebellum should be different between animal species. In the normal rat brain cerebellar TSPO is reported to be negligible or one of the lowest among brain regions. In contrast, experiments employing mice are consistently reporting higher uptake of TSPO radioligands in cerebellum together with olfactory bulb [16, 17, 31]. In the present article [^{11}C]CB184 showed almost same performance as our previous compound [^{11}C]CB148 from regional brain distribution (Fig. 3) and from the blocking experiment (Table 3). Suppressed uptake of [^{11}C]CB190 along with pretreatment with cold PK11195 was found in limited areas in spite these two compounds share the similar TSPO binding affinity and partition coefficient. It is noteworthy that partition coefficients obtained by shaking-flask method and by CLOGP program calculation showed great difference. This situation is in accordance with our previous report [24]. At present we can not define the reason for this, however, the importance of direct measurement of partition coefficient was highlighted, again.

A rat-PET study in an injured brain model enabled more adequate expectation of feasibility of the radioligand in

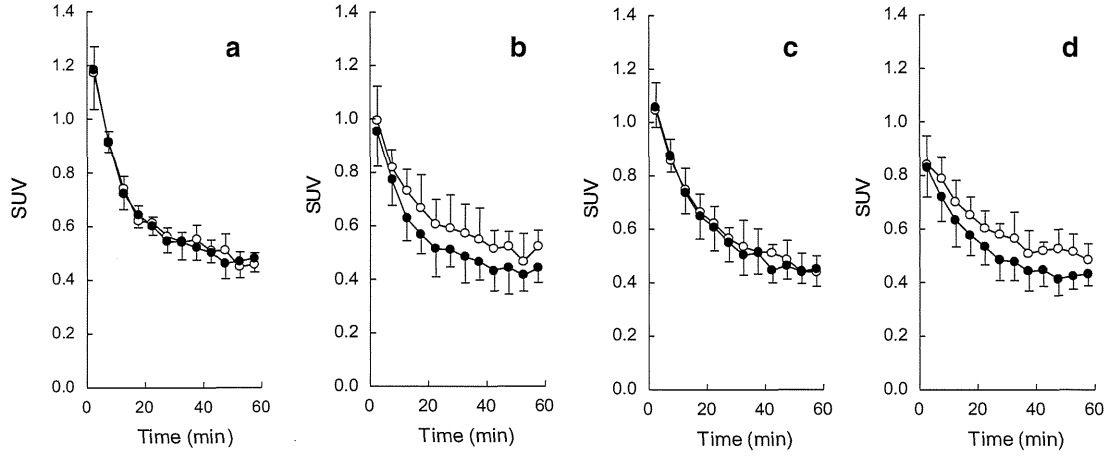

Fig. 4 Time-activity curves after i.v. injection of [^{11}C](*R*)-PK11195 or [^{11}C]CB184 to 6-OHDA lesioned rats; standardized uptake value (SUV) after intravenous injection of [^{11}C](*R*)-PK11195 (**a**, **b**) or [^{11}C]CB184 (**c**, **d**) into control (**a**, **c**) or 6-OHDA injured rat (**b**, **d**) are shown. *Open circle* shows *right* (injured) striatum and *closed circle* shows contralateral (*left*) striatum. Data are expressed as SUV (mean and SD of four animals)

Table 5 Doses of radioligands used in animal PET studies

	Radioactivity (MBq)	Pharmacological dose (nmol)		
		Total (*n*)	Low dose group (*n*)	High dose group (*n*)
[^{11}C](*R*)-PK11195	28.9 ± 6.6	2.41 ± 4.11 (9)	0.36 ± 0.28 (4)	4.45 ± 5.25 (5)
[^{11}C]CB184	29.1 ± 5.6	1.39 ± 1.96 (10)	0.19 ± 0.11 (5)	2.60 ± 2.23 (5)

Radioactivity and pharmacological dose of [^{11}C](*R*)-PK11195 and [^{11}C]CB184 were indicated. Data represent mean and SD. Number of animals was shown in the parenthesis

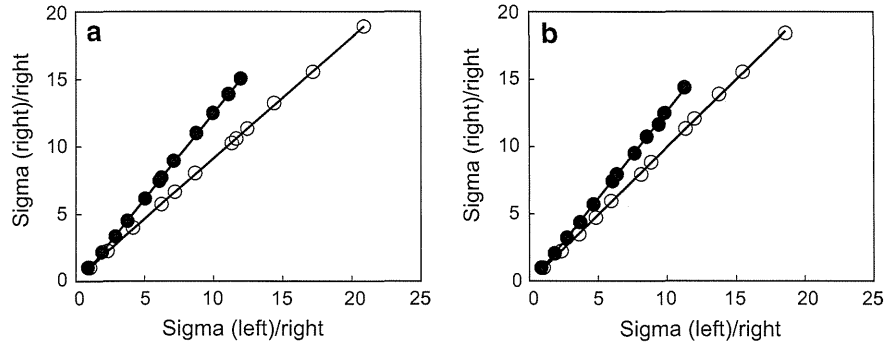

Fig. 5 Logan plot analysis; representative indirect Logan plot analysis [28, 29] of *right* and *left* striatal uptake of control (*open circle*) or 6-OHDA injured (*closed circle*) rat after intravenous injection of [^{11}C](*R*)-PK11195 (**a**) or [^{11}C]CB184 (**b**) in a rat. The analyses were carried out employing uptake of the lesioned side as target and the contralateral side as reference. After linear regression of the each plot, distribution volume ratio (DVR) between *right* and *left* striatum was obtained from its slope (see text)

patients with neurodegenerative disease. Figure 4 clearly shows that the 6-OHDA injured striatum has more uptake of TSPO tracers compared to contralateral side. Visual inspection of Fig. 4 reveals that [^{11}C]CB184 has slower washout from the rat brain than [^{11}C](R)-PK11195 due to higher binding affinity of the compound in either control or injured tissue. This tendency was in accordance with the result of mouse experiment (Fig. 3).

As TSPO is thought to exist even in normal brain tissue, the contrast between lesioned and normal brain tissue as shown in Fig. 4 does not indicate specific binding of the tracer to TSPO. It might only indicate the lesion-related

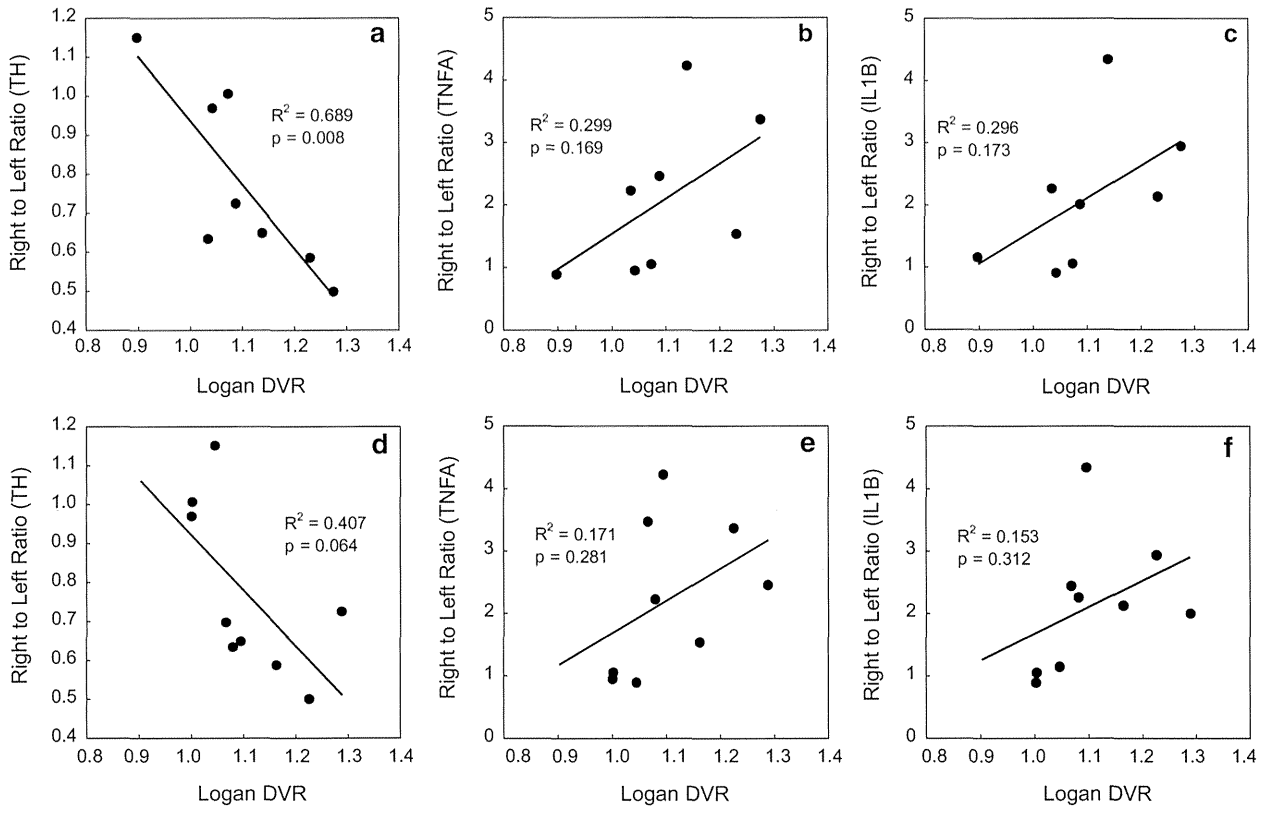

Fig. 6 Correlation between Logan DVR and *right* to *left* ratio of histochemical measures; correlation between Logan DVR and *right* to *left* ratio of number of tyrosine hydroxylase (TH) positive cell (**a**, **d**), of mRNA expression of tumor necrosis factor α (TNFA) (**b**, **e**) or interleukin-1β (IL1B) (**c**, **f**) after intravenous injection of [^{11}C](*R*)-PK11195 (**a–c**) or [^{11}C]CB184 (**d–f**) was examined. Both data from control and 6-OHDA reated rats were plotted. mRNA expression level (TNFα and IL-1β) was normalized by expression of NADPH. Data were analyzed for their correlation with Fisher's transformation. ($n = 9$ and 10 for [^{11}C]CB184 and [^{11}C](*R*)-PK11195, respectively). Regression coefficient (R^2) and critical value (p) are shown

elevation of inflammatory activity. Converse et al. [28] reported an indirect Logan plot analysis for [^{11}C](*R*)-PK11195 employing contralateral brain tissue as a reference region [29]. We also attempted this analysis and fair plot fitting and adequate DVR was obtained for both [^{11}C]CB184 and [^{11}C](*R*)-PK11195 (Fig. 5). 6-OHDA treated animals showed significantly higher DVR than non-lesioned animals for both [^{11}C]CB184 and [^{11}C](*R*)-PK11195 and the DVR shows the lesion-related elevation of inflammatory activity. DVR in 6-OHDA treated rat was 1.15 ± 0.10 for [^{11}C](*R*)-PK11195 and was 1.15 ± 0.09 for [^{11}C]CB184. These values showed no difference from ANOVA analysis and, therefore, sensitivity to detect neuroinflammation activity was similar for these two compounds.

Although we tried serial two PET scans from one batch of the each tracer, the two different pharmacological doses shown in Table 5 did not affect striatal uptake of both tracers (data not shown). As those high doses ranged from 1.3 to 6.6 nmol (from 1.6 to 7.8 μg/kg) high-end values should be regarded as maximum dose limit ensuring reproducible measurement due to low receptor occupancy. Boutin also reported that 23.7 nmol of [^{11}C](*R*)-PK11195 did not affect significantly the TACs or the contrast between the ipsilateral and contralateral side or the binding potential values [32]. Our result is in good accordance with this report.

In vivo metabolism studies showed that 36 and 25 % of radioactivity in plasma remained unchanged 30 min after intravenous injection of [^{11}C]CB184 and [^{11}C]CB190, respectively, (Table 6). It is clear contrast to the observation of [^{11}C]CB148 on which 83 % of radioactivity was observed unchanged by the same experimental system [24]. This could be explained from the difference in labeling position. As these three compounds share the *N*-dialkylacetamide substructure, a rather stable feature of [^{11}C]CB148 will explain resistance of this structure toward metabolism, however, a small amount (5 %) of polar

Table 6 Metabolite analysis

	[^{11}C]CB184		[^{11}C]CB190	
	Extraction yield (%)	Unchanged form (%)	Extraction yield (%)	Unchanged form (%)
Plasma	80.3 ± 3.3	36.2 ± 15.5	96.6 ± 3.3	25.6 ± 7.1
Brain	99.6 ± 0.1	92.7 ± 5.8	99.7 ± 0.3	86.5 ± 2.8

Data represent means and SD of three animals

metabolite was found in the brain [24]. On the other hand, polar metabolite in brain tissue was negligible for either [^{11}C]CB184 or [^{11}C]CB190.

Finally, we examined the relationship between DVR of [^{11}C](*R*)-PK11195 or [^{11}C]CB184 and histochemistry measures. We counted TH positive cells and quantified expression of inflammatory cytokines, TNFα and IL-1β mRNA by RT-PCR (Fig. 6) following our previous report [10]. We only could detect significant relationship between [^{11}C](*R*)-PK11195 DVR and left-to-right ratio of number of TH positive cells. Almost the same results were obtained when we employed right-to-left ratio of SUV value from 30 to 60 min after injection of an either radioligand (data not shown). Tight relationship between the histochemistry measures and the uptake of TSPO ligand could not be exhibited in the present examination because of limited statistical power. However, the direct comparison of PET results and inflammation indexes which can only be obtained by animal experiment will provide information concerning mechanisms underlying neurodegeneration and TSPO activation.

Recently, Yasuno et al. [33] reported that phonoxyphenyl acetamide, [^{11}C]DAA1106 binding to TSPO was significantly increased in widespread areas in subjects with mild cognitive impairment which is a prodromal state of Alzheimer's disease and this increased binding could be utilized to predict development of dementia. But a recent clinical PET study using [^{11}C]PBR28 has reported that 14 % of healthy volunteers did not have a specific binding signal in either the brain or the peripheral organs [34]. This individual difference of binding was not observed for [^{11}C](*R*)-PK11195 [35] and the similar controversy should be expected for structurally related [^{11}C]PBR06, [^{18}F]FEPPA as well as DAA family compounds. So another candidate of TSPO ligand with different structural class should be desirable also from this viewpoint.

In conclusion, we report synthesis of two carbon-11 labeled imidazopyridines TSPO ligands, [^{11}C]CB184 and [^{11}C]CB190, for PET imaging of neuroinflammation. These compounds were readily prepared by *O*-methylation reaction using [^{11}C]methyl triflate. In mice, [^{11}C]CB184 showed more uptake and specific binding than [^{11}C]CB190. In PET study using 6-OHDA treated rats, lesioned side of the brain showed higher uptake than contralateral side after i.v. injection of either [^{11}C]CB184 or [^{11}C](*R*)-PK11195. Indirect Logan plot analysis revealed distribution volume ratio (DVR) between the two sides which might indicate lesion-related elevation of TSPO binding. DVR in 6-OHDA treated mouse was 1.15 ± 0.10 for [^{11}C](*R*)-PK11195 and was 1.15 ± 0.09 for [^{11}C]CB184. These values indicate that the sensitivity to detect neuroinflammation activity was similar for these two compounds.

Acknowledgments The authors would like to thank the members of National Center for Geriatrics and Gerontology for their help. This work was supported by the Research Funding for Longevity Sciences from National Center for Geriatrics and Gerontology, Japan (21-5). All the authors disclose to have no potential conflict of interest.

References

1. Papadopoulos V, Baraldi M, Guilarte TR, Knudsen TB, Lacapère JJ, Lindemann P, et al. Translocator protein (18 kDa): new nomenclature for the peripheral-type benzodiazepine receptor based on its structure and molecular function. Trends Pharmacol Sci. 2006;27:402–9.
2. Culty M, Li H, Boujrad N, Amri H, Vidic B, Bernassau JM, et al. In vitro studies on the role of the peripheral-type benzodiazepine receptor in steroidogenesis. J Steroid Biochem Mol Biol. 1999;69:123–30.
3. Szabo I, De Pinto V, Zoratti M. The mitochondrial permeability transition pore may comprise VDAC molecules. II. The electrophysiological properties of VDAC are compatible with those of the mitochondrial megachannel. FEBS Lett. 1993;330:206–10.
4. Golani I, Weizman A, Leschiner S, Spanier I, Eckstein N, Limor R, et al. Hormonal regulation of peripheral benzodiazepine receptor binding properties is mediated by subunit interaction. Biochemistry. 2001;40:10213–22.
5. Beurdeley-Thomas A, Miccoli L, Oudard S, Dutrillaux B, Poupon MF. The peripheral benzodiazepine receptors: a review. J Neuro Oncol. 2000;46:45–56.
6. Lacapere JJ, Papadopoulos V. Peripheral-type benzodiazepine receptor: structure and function of a cholesterol-binding protein in steroid and bile acid biosynthesis. Steroids. 2003;68:569–85.
7. Banati RB. Visualizing microglia activation in vivo. Glia. 2002;40:206–17.
8. Venneti S, Lopresti B, Wiley CA. The peripheral benzodiazepine receptor in microglia: from pathology to imaging. Prog Neurobiol. 2006;80:308–22.
9. Kreutzberg GW. Microglia; a sensor for pathological events in the CNS. Trends Neurosci. 1996;19:312–8.
10. Ito F, Toyama H, Kudo G, Suzuki H, Hatano K, Ichise M, et al. Two activated stages of microglia and PET imaging of peripheral benzodiazepine receptors with [^{11}C]PK11195 in rats. Ann Nucl Med. 2010;24:163–9.
11. Shah F, Hume S, Pike V, Ashworth S, McDermott J. Synthesis of the enantiomers of [*N*-methyl-^{11}C]PK 11195 and comparison of